

JAAS

Accepted Manuscript



This is an *Accepted Manuscript*, which has been through the Royal Society of Chemistry peer review process and has been accepted for publication.

Accepted Manuscripts are published online shortly after acceptance, before technical editing, formatting and proof reading. Using this free service, authors can make their results available to the community, in citable form, before we publish the edited article. We will replace this *Accepted Manuscript* with the edited and formatted *Advance Article* as soon as it is available.

You can find more information about *Accepted Manuscripts* in the [Information for Authors](#).

Please note that technical editing may introduce minor changes to the text and/or graphics, which may alter content. The journal's standard [Terms & Conditions](#) and the [Ethical guidelines](#) still apply. In no event shall the Royal Society of Chemistry be held responsible for any errors or omissions in this *Accepted Manuscript* or any consequences arising from the use of any information it contains.



Journal Name

ARTICLE

Determination of relative rare earth element distributions in very small quantities of uranium ore concentrates using femtosecond UV laser ablation – SF-ICP-MS coupling

Received 00th January 20xx,
Accepted 00th January 20xx

DOI: 10.1039/x0xx00000x

www.rsc.org/

A. Donard,^{a,b} A.-C. Pottin,^b F. Pointurier,^b and C. Pécheyran^a

An alternative analytical method has been developed to determine lanthanide distribution using hundreds of nanograms of uranium ore concentrate (UOC) by femtosecond ultra-violet laser ablation coupled to inductively coupled plasma sector-field mass spectrometry (fs-UV-LA-ICP-SF-MS). Commonly performed from macroscopic sized samples by standard wet plasma nebulisation ICP-MS, the method developed in this study, reduces the amount of sample necessary for analysis by at least three orders of magnitude. As ablation of micrometric particles produces a short transient signal (5-10s) optimisation of the method to process such signals is discussed. Absolute limits of detection for the measurement of the 14 lanthanides were in the range of 80 to 630 attograms, allowing elemental concentrations close to the ppm to be measured in such a small quantity of UOC. Validation of the method was performed by determining the relative distribution of lanthanides in the standard UOC certified reference material, "Bolet" (CETAMA), for which concentrations of 3 lanthanides are certified. The method was also applied to the measurement of the 14 lanthanides in a UOC called "Olympic Dam". Results were in good agreement with results obtained by two laboratories for the same sample with a standard wet plasma nebulisation ICP-MS method after chemical purification (U matrix elimination and lanthanide concentration starting from macroscopic amounts of material) and with data from literature concerning the lanthanide distribution in the original U-ore.

Introduction

With the increase in illicit trafficking of nuclear material in the 1990s, a new analytical science called nuclear forensic science has emerged. Nuclear forensic science aims at providing information (origin and intended use) on seized, illegal nuclear material. This information is essential for enhancing security and preventing future loss or theft.¹⁻³ Over the past decades, several parameters have been investigated to identify signatures of the material's history.

Uranium ore concentrate (UOC) is obtained after the first step of uranium ore purification usually performed at the ore extraction site. UOCs are then transported to nuclear facilities where the uranium purification – concentration process continues. Identification of markers in UOC is essential because of the risk of loss or theft of such nuclear material. Several cases of seizures of UOCs have occurred in the past few years.⁴⁻⁶ In 2003, nearly 3 kg of radioactive material was detected in a shipment of scrap metal in Rotterdam. Nuclear

forensic experts from the Institute of TransUranium elements (ITU, Karlsruhe, Germany) have been in charge of identifying the potential source by different methods. They emphasize the importance of finding as many key parameters as possible to identify and decrease the level of uncertainty of the provenance.⁴ To characterize seized material, signatures of anthropogenic activities (chemical or physical operations) or radiogenic parameters are investigated. Identification of processes applied to UOC can for instance be carried out by measuring the non-volatile organic compound by GC-MS⁷ or determining lead isotopic composition⁸. The isotopic composition of several non-radioactive elements (Pb, Sr, O, Nd, and S)⁹⁻¹³ are also potential indicators of the UOC origin. Measurement of impurity compositions in UOCs combined with statistical treatment (principal component analysis (PCA), Soft Independent Modeling of Class Analogy (SIMCA)¹⁴, canonical analysis of principal coordinates (CAP)¹⁵) allows the classification of a UOC according to its type of original deposit. Among all of these indicators, rare earth element (REE) composition (i.e. distribution of the relative abundances of REEs) is a very interesting candidate for origin deposit determination.^{16,17} The REE distribution can be regarded as a characteristic of the types of uranium deposit. The REE pattern is directly related to the mineralizing process and geological settings.¹⁸ For example, no fractionation between the REEs is characteristic of an intrusive and a synmetamorphic deposit.¹⁹ REEs are incorporated during the ore formation and unlike

^a Laboratoire de Chimie Analytique Bio-Inorganique et Environnement, UMR 5254, Hélioparc Pau-Pyrénées, 2 Avenue du Président Angot, 64053 Pau, France. E-mail: Christophe.Pecheyran@univ-pau.fr; Fax: +33.559.407.781; Tel: +33.559.407.757

^b CEA/DAM-DIF/DASE/SRCE, PO Box 12, 91680 Bruyères-le-Châtel, France.

Electronic Supplementary Information (ESI) available: [details of any supplementary information available should be included here]. See DOI: 10.1039/x0xx00000x

1
2
3
4
5
6
7
8
9
10
11
12
13
14
15
16
17
18
19
20
21
22
23
24
25
26
27
28
29
30
31
32
33
34
35
36
37
38
39
40
41
42
43
44
45
46
47
48
49
50
51
52
53
54
55
56
57
58
59
60

other parameters such as U, Pb, O, isotopic compositions are less sensitive to post-depositional re-equilibration.¹⁸ In addition, the milling process applied to transform ore into ore concentrate does not seem to modify the REE distribution allowing the possibility to link a UOC to its deposit of origin.¹⁷ To fully exploit this indicator, it is necessary to build a comprehensive database of measurements of the REE distribution in several specimens from the various types of deposit. A drawback is that, as mentioned by Bürger et al.,²⁰ no certified reference material for lanthanides is currently available. However, the relevant information for nuclear forensics is mainly the REE distribution (i.e. relative concentrations) and not the absolute concentrations.

Regarding the analytical techniques, inductively coupled plasma mass spectrometry (ICP-MS) has been used recently as an effective technique for the determination of the lanthanide distribution in UOC,^{5,21,20} even though lanthanides are present at trace levels ($\mu\text{g}\cdot\text{g}^{-1}$ or less). Samples can be analyzed directly after digestion and dilution,^{5,20,22} or lanthanides can be separated from the uranium matrix by oxalate precipitation and solvent extraction²³ as well as by chromatography using, for instance, an extraction chromatography TRUTM resin.²¹ Depending on the relative concentrations of the matrix and lanthanides, spectral interferences may cause bias in the results. $^{238}\text{U}^{40}\text{Ar}^{2+}$ can interfere with Lanthanum (^{139}La); in the m/z region, from 140 to 170 atomic mass units, it can be disturbed by oxide and hydroxide molecular ions of barium.²¹ Interference could be resolved by using a high mass resolution mode, for example, ICP-MS equipped with double focalization of the ion beams using electrostatic and magnetic fields (ICP-SF-MS where SF stands for "sector field"). The use of a high mass resolution implies a significant loss of sensitivity and due to the low REE concentrations in UOCs this solution is inappropriate. Matrix separation improves the detection limit by two orders of magnitude, and protects the instrument from uranium contamination.²¹ However, these methods are time-consuming and generate uranium-containing effluents. Except if the laboratory has at its disposal isotopic dilution tracers for the REEs, chemical yields for the different REEs are not known, which may bias the REE distribution. Combination of all the uncertainties in each of the various steps: (concentration measurement, weighing, chemical recovery, etc.) may lead to high uncertainty levels.

Direct analytical methods, which do not require extensive preparation and manipulation, which do not generate waste and also minimize the possible sources of contamination, are obviously of great interest. In the scope of nuclear forensic science the quantities of sample available for analysis can be an issue. The quantity of seized nuclear material is often limited.²⁴ It may also be necessary to divide the seized material into several sub-samples to perform different analyses, which are often destructive, as well as to keep a part of the seized material as an archive and/or for further analysis. Therefore, it is of great interest to be able to use as low as possible mass of material for the analysis. To perform analysis by ICP-MS after matrix separation, several milligrams of sample are needed to detect lanthanide above the limit of detection.²¹ The use of

laser ablation (LA) as sample introduction mode for direct ICP-MS detection without matrix separation drastically lowers the amount of sample required for the measurement. Analyses by LA-ICP-MS coupling are fast, do not generate effluents, as no chemical preparation is required, and can provide spatial information. It has been shown that analysis of micrometric particles by LA-ICP-MS coupling, produces very short transient signals with high signal/noise ratios leading to very low detection limits.²⁵⁻²⁷ Most importantly, if analysis can be performed at the scale of individual particles of a few μm in size, several UOCs of different origins could be identified in the case of a mixing of UOCs. For example, the trace element abundance was measured starting from a relatively high amount of material in a UOC seized in South Africa, which did not correspond to any uranium ore in the database. X-ray diffraction performed on the sample revealed that 4 phases were present in the UOC. Thus, "bulk analysis" led logically to a mixed REE distribution.⁶

In this study, determination of the lanthanide distribution in UOC particles was undertaken by an UV-femtosecond laser coupled with an ICP-SF-MS. The LA-ICP-MS technique has already been successfully used for the determination of REE distribution in uranium ore at a microscopic level^{18,28}. It has not yet to our knowledge, been used for microscopic amounts of UOC for which REE concentrations can be several orders of magnitude lower than those in U-ores. Only the relative distribution of lanthanides in UOCs was determined in this study as this information is sufficient to link the UOC and the deposit of origin. Methodology was developed with the reference material "Bolet" (CETAMA, Marcoule, France) certified for 3 lanthanides (Eu, Sm, Dy) and applied to a UOC from the "Olympic Dam" ore mill in Australia. Results were compared to the lanthanide distributions measured by two different laboratories (CEA and ITU) using liquid solution introduction mode ICP-MS after matrix separation, and with the REE distribution reported in the literature for the "Olympic Dam" ore.²⁹

Material and methods

Sample preparation

The U_3O_8 certified reference material "Bolet" (CETAMA, Marcoule, France) was used for the optimization of the method. Concentrations of 3 lanthanides: Sm, Eu, and Dy, were certified with respective concentrations of 0.19, 0.18 and $0.17 \mu\text{g}\cdot\text{g}^{-1}$. It should be mentioned that these three elements were added to the UOC and that the resulting concentrations are higher than the ones encountered in UOCs, which makes "Bolet" an ideal material for method optimization. A real life UOC from the Australian uranium deposit "Olympic Dam" was also analyzed to validate the methodology. Both UOCs were in powder form and the following sample preparation was applied; a small amount of particles representing a few μg of uranium, were dispersed in a mixture of collodion (4% nitrocellulose in ether-alcohol media, Merck) and ethanol, and deposited on 3 cm diameter polycarbonate disks. After

evaporation of the ethanol, the particles were fixed in the collodion layer a few μm thick.

For the analysis in liquid solution introduction mode at ITU and CEA, particles were dissolved in nitric acid and separation from the matrix was performed by extraction chromatography following the procedure described elsewhere.²¹

Instrumentation

The LA-ICP-MS measurements were carried out using an ICP-SF-MS “Element XR” (Thermo Scientific, Bremen, Germany) coupled with a UV-femtosecond laser ablation system “Lambda 3” (Nexeya SA, Canejan, France). This laser is fitted with a diode-pumped Yb:KGW crystal laser source (HP2, Amplitude system, Pessac, France). Three wavelengths can be selected, 1030 nm (fundamental), 515 nm (2nd harmonic) and 257nm (4th harmonic). The 257 nm wavelength was used in this study as described elsewhere.³⁰ The laser source operates within a wide range of repetition rates (1Hz-100 kHz) and at low energy (from 200 μJ per pulse below 1 kHz to 1.5 μJ at 100 kHz). The laser beam can be moved rapidly by the use of 2D galvanometric scanners (up to 2 $\text{m}\cdot\text{s}^{-1}$). The aerosols generated from the ablation of the particles were carried to the ICP-MS by helium as a vector gas. The Element XR used for all the measurements is equipped with the “Jet interface”, i.e. special sampler cones and an additional pump, which strongly enhance sensitivity by a factor of ~ 3 -5 for liquid nebulization ICP-MS. All the measurements were carried out in low-resolution mode ($R=300$) to keep on full transmission inside the mass analyzer. Nitrogen was added to the helium flow by a Y connection (10mL/min). Mixing of N_2 with Ar enhanced sensitivity for elements in the high mass ranges.³¹⁻³³ The coupling was performed in dry plasma conditions. Ablation of transect in glass standard CRM NIST 612 was used on a daily basis to optimize the parameters of the ICP-MS to ensure high sensitivity and good stability (relative standard deviation of the signals for ^{238}U and ^{232}Th were below 3% for 20 points in a row). To ensure complete atomization and ionization efficiency of the plasma, parameters were adjusted to keep the $^{238}\text{U}/^{232}\text{Th}$ ratio as close as possible to 1 ± 0.05 .^{34,35}

As mentioned before, results obtained with LA-ICP-MS were compared with those obtained by CEA and ITU after matrix separation and REE purification using extraction chromatography and liquid solution introduction mode ICP MS, also using ICP-SF-MS, (respectively “Element 2” and “Element XR”, Thermo Scientific, Bremen, Germany). Analytical conditions used by ITU are described elsewhere.²¹

Ablation parameters and data acquisition

Each polycarbonate disk was fixed in the ablation cell with a small piece of double-sided tape. Ablations of the particles were carried out by combining a high repetition rate (1 kHz) and the rapid movement of the galvanometric scanners (1 mm/s) to produce a resulting ablation spot with a diameter of 100 μm on the disk. For development and optimization of the analytical procedure with the “Bolet” reference material, only the signals corresponding to the 3 lanthanides with certified

concentrations were recorded (La, Dy, Eu). For the “Olympic Dam” UOC, signals for at least one isotope of each one of the 14 REEs were recorded.

The challenge of this study is to measure the relative distribution of the lanthanides present as impurities in UOC particles using only very small quantities of material, representing typically hundreds of nanograms of uranium and consequently femtograms of each REE. The signal thus obtained is very low, short and transient (only a few seconds). The SF-ICP-MS “Element XR” used here is suitable for this application because of its extremely high sensitivity. However, the use of this type of instrument has one drawback: the stabilization time of the magnetic field after a change of the value of the magnetic field (< 300 ms) is too long with respect to the total duration of the LA-ICP-MS signal. To prevent loss of a significant part of the detection time, the magnetic field value was kept constant during the whole acquisition. As a consequence, the mass scan was performed by only using electrostatic scanning (for which stabilization time of only 1 ms per m/z). This however strongly limits the analyzed mass range to $\pm 17\%$ of the mass spectrum around the central m/z ratio. Under these conditions, the uranium signal that was proven by Lach et al.²⁸ to be a good internal standard to quantify REE content in uranium oxide by LA-ICP-MS was not recorded because the mass gap was too large to be covered by the electrostatic scanning. However, the mass range allowed by electrostatic scanning is sufficient to measure all the REEs of interest.

Data was acquired as raw counts per second (cps) for 80 s. The blank signal was measured for 20 s before the beginning of the ablation. Ablation and data acquisition parameters are reported in Table 3.

Data processing

The baseline estimated by the average signal measured during the 20 seconds prior to the ablation was subtracted point by point from the signals measured for each isotope in the ablation peak. Blank polycarbonate disks coated with collodion were ablated to check for absence of contamination in the matrix. Blank count rates were negligible for all of the lanthanides as they were not significantly higher than the baseline recorded prior to ablation. Signal intensities were integrated over the ablation time for each REE and the elemental ratios of interest were calculated according to the following equation (after calibration using NIST 612):

$$\frac{[E^1]_{\text{sample}}}{[E^2]_{\text{sample}}} = \frac{N(E^1)_{\text{sample}}}{N(E^2)_{\text{sample}}} \times \frac{[E^1]_{\text{NIST612cert}} \times N(E^2)_{\text{NIST612cert}}}{[E^2]_{\text{NIST612cert}} \times N(E^1)_{\text{NIST612cert}}}$$

Where $[E^i]_{\text{sample}}$ is the concentration of the lanthanide in the sample, $[E^i]_{\text{NIST612cert}}$ is the certified concentration of the lanthanide in the NIST 612 reference material, $N(E^i)_{\text{sample}}$ the integrated number of counts for the ablation of the lanthanide in the sample, and $N(E^i)_{\text{NIST612meas}}$ the integrated number of counts for the ablation of the lanthanide in the NIST SRM 612. Although limited elemental fractionation is generally reported

for most of the rare earth elements³⁶, some authors³⁷ have pointed out more significant elemental fraction with respect to La using 213 nm nanosecond laser. As demonstrated by several authors the use of the femtosecond laser leads to an efficient reduction of fractionation effects and therefore offers the possibility of accurate non-matrix matched analysis.³⁸⁻⁴¹

Results and discussion

Optimization of the method

The challenge of this method is the very small quantity of analyte available to perform the measurement. Lanthanides are present as trace elements in UOC (typically between the ng.g^{-1} and the $\mu\text{g.g}^{-1}$ levels) and for each ablation only a few particles of UOC of a few μm in size are analyzed, typically representing hundreds of nanograms of uranium. For example, in a 10 μm diameter particle of “Bolet” equivalent to a dense sphere, the quantity of Sm would represent approximately 800 ag (according to the concentration of 0.19 $\mu\text{g.g}^{-1}$ given in the certificate). The LA-ICP-MS signal, which is highly transient, short (approximately 5s) in the case of the analysis of dispersed particulate material, is also of low intensity. Figure 1 presents an example of an ablation of “Bolet” particles dispersed on a polycarbonate disk.

With such signals, special care has to be taken with data acquisition. The total measurement time t_T is given by:

$$t_T = n_C \times \sum_{i=1}^{n_i} (n_{pp_i} \times t_{D_i} + t_{S_i})$$

Where n_C is the number of measurement cycles, n_i the number of isotopes, n_{pp_i} is the number of points per peak recorded for the isotope i , t_{D_i} is the counting time for the individual measurement of the isotope i (called “Sample Time”), and t_{S_i} is the stabilization time of the instrument after a mass jump (“settling time”). In our case, the mass scan was operated using the electrostatic analyzer only, so the settling time was the same for all isotopes (t_S). If the sample time and the number of points per peak are identical for all isotopes, then the previous formula becomes:

$$t_T = n_C \times n_i \times (n_{pp} \times t_D + t_S)$$

The total measurement time is defined by the analyst and corresponds to the duration of the ablation peak on which the signals are integrated.

The counting time t_M for each isotope is:

$$t_M = n_C \times n_{pp} \times t_D$$

The counting time must be optimized by maximizing its ratio to the total measurement time:

$$r = \frac{n_{pp} \times t_D}{n_i \times (n_{pp} \times t_D + t_S)}$$

The highest ratios are obtained by minimizing the number of isotopes, but also by having a much longer sample time with

respect to the settling time, which is 1 ms in the case of this study.

However, a dwell time that is too long raises the risk of spectral skew.^{42,43} Spectral skew arises when a transient signal is measured with sequential acquisition. If the time of measure for each isotope is too long in comparison to the total measurement time, the resulting peak integrated per isotope is not representative of the actual arrival of isotope in the detector (cf Figure in supplementary information).

Pettke et al.⁴³ demonstrated that for two different dwell times (5 ms and 10 ms) in a single shot experiment performed by LA-ICP-MS, the effect of spectral skew is negligible on the precision when more than 30 measurements are recorded for each ablation peak, i.e. more than 30 measurement cycles over the duration of the ablation peak.

The reference material “Bolet” is a relevant choice for testing and validating the developed procedure because the three certified REEs (Sm, Eu, Dy) are relatively abundant and were simultaneously added to the material using a thorough homogenization process. In the following, we assume the relative concentrations of these three elements are homogeneous at the scale of the small quantity being analyzed. In Figure 2 the relative standard deviations (RSDs) obtained for different dwell times (defined here as $n_{pp.t_D}$) and calculated from 12 ablations of very small amounts of “Bolet” are compared to the theoretical RSDs calculated from counting statistics according to Poisson’s law. From 1 ms to 100 ms, experimental RSDs were consistent with theoretical values. However, for 500 ms and 1 s, experimental RSDs were not in agreement with theoretical RSDs. The number of individual measurements (number of dwell times) for each isotope are given in Table 2. For dwell times of 500 ms and 1 s, the signals are respectively defined by 7 and 3 individual measurements over the whole ablation peak, which is obviously too low. The reproducibility is thus affected by spectral skew.

For the determination of the REE distribution in a real UOC, 14 lanthanides should be measured, and not only three of them. A low value of 10 ms was chosen for the dwell time in order to keep the number of measurements above 30.

Limit of detection

Limits of detection (LODs) were determined by performing 26 ablations on two blank disks. Blank disks were prepared following the same protocol employed to fix the particles, i.e. mixtures of collodion and ethanol were deposited on polycarbonate disks. During the integration time, the total number of counts was lower than 70 counts. Under these conditions, the normal distribution hypothesis commonly used to calculate the LODs ($3 \times \text{SD}$) is not true and would give inconsistent and low LODs, the model based on the Poisson Statistics being more appropriate.⁴⁴ The absolute detection $L(E)_{\text{Abs}}$ for the element E , expressed in μg , was estimated as follow:

$$L(E)_{\text{Abs}} = \frac{2.71 + 3.29 \times \sqrt{N(E)_{\text{Blank}}}}{S(E)}$$

With $N(E^i)_{Blanks}$, the number of integrated counts in the blank disks and $S(E)$ the sensitivity for the element E (counts μg^{-1}). The sensitivity was determined by performing a crater in the reference glass material NIST 612, and calculated according to the following formula:

$$S(E) = \frac{N(E^i)_{NIST}}{[E]_{NIST} \times V \times \rho}$$

Where $N(E^i)_{NIST}$ is the integrated number of counts of the isotope i for the element E in the NIST SRM 612, $[E]_{NIST}$ the concentration of the element E in the NIST SRM 612 ($\mu\text{g}\cdot\text{g}^{-1}$), V the ablated volume (cm^3) and ρ is the volumetric mass of the NIST SRM 612 ($\text{g}\cdot\text{cm}^{-3}$).

The volume ablated was measured by rugosimetry (Micromesure Table and CH150 captor, STIL., Aix en Provence, France). Table 3 presents the relative limit of detection in absolute values, calculated from the blank disks. For micro-analysis, absolute limit of detection corresponds to the minimum detectable⁴⁵ mass of analyte. In this study, low absolute limits of detection ranging from 80 to 700 attograms were obtained. This wide range is mostly attributed to the relative isotope abundance of the element of interest and to a lesser extent to blank values. Note that using this Poisson statistical assumption, LODs for blank values very close to zero are still questionable since even if blank values were equal to zero, the LOD would be equal to $2.71/S(E)$, roughly 2 to 3 times lower than our values (see Table 3).

In comparison, Varga et al.²¹ published low limits of detection in the tens of ppb range corresponding to absolute detection limits between 0.02 and 2 μg for 13 mg of uranium after matrix separation and REE extraction. If we consider the "Olympic Dam" UOC for which Sm concentration estimated by Keegan et al.²² (by ICP-MS measurement) was 10 $\text{ng}\cdot\text{g}^{-1}$, Sm can be theoretically detected by fs-UV-LA-SF-ICP-MS in a particle of 20 μm corresponding to 38 ng of UOC (with a theoretical dense sphere shape of $8380 \text{ kg}\cdot\text{m}^{-3}$).

Validation of the method

To validate the methodology, elemental ratios measured in the reference material "Bolet" were compared with the certified values. "Bolet" is certified for the three lanthanides Sm, Dy, and Eu. To our knowledge, no reference material of UOC certified for all 14 REEs is available²⁰. The chemical properties for this class of elements are very similar but some elements are more or less affected by interference. Figure 3 compares the elemental ratios measured in micro-sized particles of "Bolet" (41 ablations of 4-20 ng of U_3O_8 equivalent to 10-17 μm) with the reference values given in the certificate. Uncertainties ($k=1$) for the measured elemental ratios are calculated from the standard deviation over the 41 ablations. To estimate the uncertainties in reference elemental ratios, the quadratic combination formula was used.

$$u\left(\frac{E_1}{E_2}\right) = \sqrt{\left(\frac{[E_1]}{u_{E_1}}\right)^2 + \left(\frac{[E_2]}{u_{E_2}}\right)^2}$$

With $u()$ the uncertainty of the ratio of the element E_1 and the element E_2 , $[E_1]$ and $[E_2]$ the concentrations of the elements E_1 and E_2 in "Bolet".

Elemental ratios measured from the ablation of low amounts of "Bolet" are in good agreement with the values given in the certificate. The relative differences with the expected elemental ratios Eu/Sm, and Dy/Sm are respectively, 5% and 2%. The uncertainties measured are between 13-16%. These uncertainties are consistent with the external reproducibility expected for the chosen method (10 ms dwell time). The theoretically achievable RSD according to Poisson law varies between 7-16% for the elemental ratios measured. No conclusion can be made from these results on the homogeneity of the material at the microscopic scale. The reference material "Bolet" is produced from pure uranium oxide, U_3O_8 , that is enriched in impurities by impregnation, suggesting that the material should be homogeneous even at the microscopic level.⁴⁶

Comparison with the result obtained by liquid ICP-MS after matrix separation

The method was applied to the analysis of a UOC from an Australian mill called "Olympic Dam". One isotope of each of the 14 lanthanides was measured during each ablation. The relative distribution of the lanthanide relative concentrations (normalized to the Sm concentration, Sm was chosen arbitrarily) measured by fs-UV-LA-SF-ICP-MS are shown in Figure 4. The distribution is compared with the ones obtained by ICP-MS after separation of the matrix by two laboratories (ITU and CEA). The uncertainties presented for fs-UV-LA-SF-ICP-MS are calculated as twice the standard deviation of 10 ablations for "Olympic Dam" ($k=2$). Each trajectory of ablation includes 3-5 particles equivalent to 100-400 ng of UOC (average for the 10 ablations). The uncertainties for the bulk methods are used for comparison.

The results of the LA-ICP-MS method are in good agreement with the results from the "bulk" method (chemical purification followed by liquid introduction ICP-MS) except for La/Sm (15.5 ± 5.1 by LA-ICP-MS versus 4.6 ± 0.6 and 7.3 ± 0.5 by "bulk" analysis respectively by CEA and ITU). These differences may be due to the interference of $^{238}\text{U}^{40}\text{Ar}^{2+}$ at $m/z = 139$. A solution to correct for this interference could be to estimate the formation rate of UAR^{2+} , to record U during the UOC ablation, to calculate the level of UAR^{2+} and to subtract the UAR^{2+} from the raw signal. However, this solution is not recommended for the ablation of very small quantities of material, because a variation of the magnetic field is necessary to measure a uranium isotope. Therefore, a settling time of 300 ms would be added for each cycle which would strongly limit the number of measurement cycles per ablation and per element. The number of measurement cycles would fall below the required 30 individual measurements for accurate measurement.

The standard deviation calculated from 10 micro-analyses varied between 22.5%-40%. The uncertainties are consistent

with the external reproducibility expected according to Poisson law (11%-40%).

Comparison with the uranium ore of origin.

Varga et al.¹⁷ have proven that the REE distribution in UOC is not modified by the purification process and presents similarities with the REE distribution of the deposit of origin. The REE distribution obtained in our study by fs-UV-LA-SF-ICP-MS in the "Olympic Dam" UOC was compared to data concerning the original ore obtained by Ciobanu et al.²⁹ They investigated the suitability of hematite for U-Pb geochronology using LA-ICP-MS coupling and measured the 14 REEs in different hematites. The REE distributions (normalized to the concentration of Sm) are presented in Figure 5. The overall shape of the distribution is similar in the ore and in the UOC, with an enrichment of the light REEs with respect to the heavy REEs.

Conclusions

A new analytical methodology has been developed to measure the relative distribution of REEs in a few hundred nanograms of uranium ore concentrate by fs-UV-LA-SF-ICP-MS. Laser ablation allows the direct measurement of the sample, no matrix separation is needed, and therefore the risk of contamination and the production of radioactive waste is diminished. Ablation of a few particles produces an extremely short and low transient signal. Reproducibility is governed by counting statistics preventing any conclusion on the homogeneity of the material at the microscopic scale. With this method, the REE relative distribution measured in a UOC from "Olympic Dam" was found to be comparable to the REE pattern of its deposit of origin. The measurement was performed from only hundreds of nanograms of UOC, a reduction of the sample uptake of a factor of a 100 000 compared to liquid nebulization mode ICP-MS. Nevertheless, the results obtained by fs-UV-LA-ICP-MS were consistent with standard nebulization wet plasma ICP-MS, except for the lanthanum that might be interfered with by UAr^{2+} in fs-UV-LA-ICP-MS. This method is of great interest for forensic studies. Analysis of uranium ore concentrate should focus on reaching the microscopic scale to be able to discriminate the components of a mixing of UOCs. Development should be done on the sensitivity of the SF-ICP-MS to lower the limit of detection and enable analysis of single particles.

Acknowledgements

The authors wish to thank H el ene Garay for crater depth measurement by rugosimetry. They also thank Zsolt Varga for data transmission and useful talks on lanthanide measurement by ICP-MS in uranium ore concentrate. Region Aquitaine and Feders are also thanked for instrument fundings.

References

- 1 K. Mayer, M. Wallenius and T. Fangh anel, *J. Alloys Compd.*, 2007, **444-445**, 50–56.
- 2 M. Wallenius, K. Mayer and I. Ray, *Forensic Sci. Int.*, 2006, **156**, 55–62.
- 3 K. Mayer, M. Wallenius and I. Ray, *Analyst*, 2005, **130**, 433–441.
- 4 B. Z. Varga, M. Wallenius, K. Mayer and M. Meppen, *Proc. Radiochim. Acta*, 2011, **4**, 1–4.
- 5 E. Keegan, M. J. Kristo, M. Colella, M. Robel, R. Williams, R. Lindvall, G. Eppich, S. Roberts, L. Borg, A. Gaffney, J. Plaue, H. Wong, J. Davis, E. Loi, M. Reinhard and I. Hutcheon, *Forensic Sci. Int.*, 2014, **240**, 111–21.
- 6 I. D. Hutcheon, in *AIEA conference on advances in nuclear forensic*, Vienna, 2014.
- 7 A. K. Kennedy, D. A. Bostick, C. R. Hexel, R. R. Smith and J. M. Giaquinto, *J. Radioanal. Nucl. Chem.*, 2013, **296**, 817–821.
- 8 A. J. Fahey, N. W. M. Ritchie, D. E. Newbury and J. A. Small, *J. Radioanal. Nucl. Chem.*, 2010, **284**, 575–581.
- 9 Z. Varga, M. Wallenius, K. Mayer, E. Keegan and S. Millet, *Anal. Chem.*, 2009, **81**, 8327–8334.
- 10 J. Švedkauskaitė-LeGore, K. Mayer, S. Millet, A. Nicholl, G. Rasmussen and D. Baltrunas, *Radiochim. Acta*, 2007, **95**.
- 11 L. Pajo, K. Mayer and L. Koch, *Fresenius. J. Anal. Chem.*, 2014, **371**, 348–352.
- 12 J. Krajk o, Z. Varga, E. Yalcintas, M. Wallenius and K. Mayer, *Talanta*, 2014, **129**, 499–504.
- 13 S.-H. Han, Z. Varga, J. Krajk o, M. Wallenius, K. Song and K. Mayer, *J. Anal. At. Spectrom.*, 2013, **28**, 1919.
- 14 J.-B. Sirven, A. Pailloux, Y. M'Baye, N. Coulon, T. Alpettaz and S. Goss e, *J. Anal. At. Spectrom.*, 2009, **24**, 451–459.
- 15 E. Keegan, M. Wallenius, K. Mayer, Z. Varga and G. Rasmussen, *Appl. Geochemistry*, 2012, **27**, 1600–1609.
- 16 K. Mayer, M. Wallenius and Z. Varga, *Chem. Rev.*, 2013, **113**, 884–900.
- 17 Z. Varga, M. Wallenius and K. Mayer, *Radiochim. Acta*, 2010, **98**, 771–778.
- 18 J. Mercadier, M. Cuney, P. Lach, M.-C. Boiron, J. Bonhoure, A. Richard, M. Leisen and P. Kister, *Terra Nov.*, 2011, **23**, 264–269.
- 19 M. Cuney and K. Kyser, *Recent and not-so-recent developments in uranium deposits and implications for exploration*, Mineralogi., 2008.
- 20 S. B urger, S. F. Boulyga, M. V. Pe rkin, D. Bostick, S. Jovanovic, R. Lindvall, G. Rasmussen and L. Riciputi, *J. Radioanal. Nucl. Chem.*, 2014, **301**, 711–729.
- 21 Z. Varga, R. Katona, Z. Stef anka, M. Wallenius, K. Mayer and A. Nicholl, *Talanta*, 2010, **80**, 1744–1749.
- 22 E. Keegan, S. Richter, I. Kelly, H. Wong and P. Gadd, 2008, **23**, 765–777.

- 1
2
3
4
5
6
7
8
9
10
11
12
13
14
15
16
17
18
19
20
21
22
23
24
25
26
27
28
29
30
31
32
33
34
35
36
37
38
39
40
41
42
43
44
45
46
- 23 A. Premadas and P. K. Srivastava, *J. Radioanal. Nucl. Chem.*, 2002, **251**, 233–239.
- 24 J. Krajko, Z. Varga, M. Wallenius and K. Mayer, *J. Radioanal. Nucl. Chem.*, 2015, **304**, 177–181.
- 25 F. Pointurier, A. Hubert and A.-C. Pottin, *J. Radioanal. Nucl. Chem.*, 2012, **296**, 609–616.
- 26 F. Pointurier, A. C. Pottin and A. Hubert, *Anal. Chem.*, 2011, **83**, 7841–7848.
- 27 A. Hubert, F. Claverie, C. Pécheyran and F. Pointurier, *Spectrochim. Acta - Part B At. Spectrosc.*, 2014, **93**, 52–60.
- 28 P. Lach, J. Mercadier, J. Dubessy, M.-C. Boiron and M. Cuney, *Geostand. Geoanalytical Res.*, 2013, **37**, 277–296.
- 29 C. L. Ciobanu, B. P. Wade, N. J. Cook, A. Schmidt and D. Giles, *Precambrian Res.*, 2013, **238**, 129–147.
- 30 M. Resano, M. Aramendía, L. Rello, M. L. Calvo, S. Bérail and C. Pécheyran, *J. Anal. At. Spectrom.*, 2013, **28**, 98–106.
- 31 T. Hirata and R. W. Nesbitt, *Geochim. Cosmochim. Acta*, 1995, **59**, 2491–2500.
- 32 S. A. Crowe, B. J. Fryer, I. M. Samson and J. E. Gagnon, *J. Anal. At. Spectrom.*, 2003, **18**, 1331–1338.
- 33 M. Aramendía, M. Resano and F. Vanhaecke, *J. Anal. At. Spectrom.*, 2010, **25**, 390.
- 34 B. Hattendorf, C. Latkoczy and D. Günther, *Anal. Chem.*, 2003, **75**, 341A–347A.
- 35 D. Günther and B. Hattendorf, *TrAC Trends Anal. Chem.*, 2005, **24**, 255–265.
- 36 B. J. Fryer, S. E. Jackson and H. P. Longerich, *Can. Mineral.*, 1995, **33**, 303–312.
- 37 K. Tanaka, Y. Takahashi and H. Shimizu, *Anal. Chim. Acta*, 2007, **583**, 303–9.
- 38 N. Miliszkievicz, S. Walas and A. Tobiasz, *J. Anal. At. Spectrom.*, 2015, **30**, 327–338.
- 39 J. Koch, H. Lindner, A. von Bohlen, R. Hergenröder and K. Niemax, *J. Anal. At. Spectrom.*, 2005, **20**, 901–906.
- 40 Q. Bian, C. C. Garcia, J. Koch and K. Niemax, *J. Anal. At. Spectrom.*, 2006, **21**, 187–191.
- 41 J. González, C. Liu, X. Mao and R. Russo, *J. Anal. At. Spectrom.*, 2004, **19**, 1165–1168.
- 42 M. Wälle and C. a. Heinrich, *J. Anal. At. Spectrom.*, 2014, **29**, 1052–1057.
- 43 T. Pettke, C. a. Heinrich, A. C. Ciocan and D. Günther, *J. Anal. At. Spectrom.*, 2000, **15**, 1149–1155.
- 44 M. Tanner and D. Günther, *Anal. Chim. Acta*, 2009, **633**, 19–28.
- 45 O. G. A. Petrucci, P. Cavalli and J. D. Winefordner, *Fresenius. J. Anal. Chem.*, 1996, **882**, 878–882.
- 46 M. Crozet, V. Dubois, P. Bros, G. Lamarque and J. Delion, in *Atalante2000*, 2000.

Journal Name

ARTICLE

LAMBDA III Laser ablation system

Laser source	Yb:KGW
Wavelength	257 nm
Pulse duration	<400 fs
Repetition rate	1000 Hz
Scanner speed	1 mm.s ⁻¹
Ablation strategies	Disk of 100 μm

Element XR ICP-SF-MS

RF Power	950 W
Cooling gas flow rate	16 L.min ⁻¹
Auxiliary gas flow rate ³	1.10 L.min ⁻¹
Nebulizer gas flow rate	0.4 L.min ⁻¹
Resolution	300
Sample per peak	60
Mass window	3%
Setting time	0.001 s
Sample time	0.005 s
Scan type	E-scan
Measured isotopes	For "Bolet": ¹⁴⁷ Sm, ¹⁵³ Eu and ¹⁶³ Dy For "Olympic Dam": ¹³⁹ La, ¹⁴⁰ Ce, ¹⁴¹ Pr, ¹⁴³ Nd, ¹⁴⁷ Sm, ¹⁵³ Eu, ¹⁵⁷ Gd, ¹⁵⁹ Tb, ¹⁶³ Dy, ¹⁶⁵ Ho, ¹⁶⁶ Er, ¹⁶⁹ Tm, ¹⁷² Yb and ¹⁷⁵ Lu

Table 1 Optimized ICP-MS and Laser operating parameters

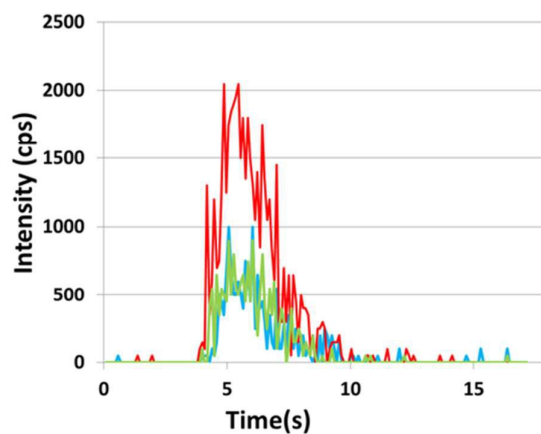


Figure 1 Example of the signals measured for the fs-UV-LA-SF-ICP-MS analysis of particles of the UOC reference material "Bolet" for the isotopes ^{147}Sm (blue line), ^{153}Eu (red line) and ^{163}Dy (green line).

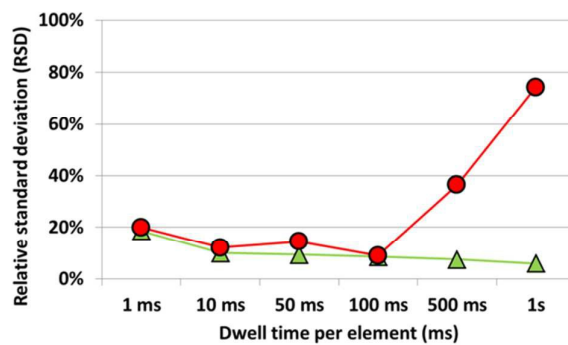


Figure 2 Comparison of the experimental (red circles) relative standard deviation (RSD) calculated for Sm/Dy of the "Bolet" material from 12 successive LA-ICP-MS analyses performed for each dwell time, with the theoretical (green triangles) RSD achievable according to the Poisson Law and starting from the measured number of counts.

Journal Name

ARTICLE

Dwell time (ms)	Number of individual measurements per isotope – measurement of 3 isotopes	Number of individual measurements per isotope – measurement of 14 isotopes
1	1667	357
10	303	65
50	65	14
100	33	7
500	7	1
1 000	3	/

Table 2 Numbers of individual measurements per isotope for an integrated ablation of 10 s depending on the dwell time

	La ¹³⁹	Ce ¹⁴⁰	Pr ¹⁴¹	Nd ¹⁴³	Sm ¹⁴⁷	Eu ¹⁵³	Gd ¹⁵⁷	Tb ¹⁵⁹	Dy ¹⁶³	Ho ¹⁶⁵	Er ¹⁶⁶	Tm ¹⁶⁹	Yb ¹⁷²	Lu ¹⁷⁵
$N(E)_{\text{Blank}}$	3	5	2	3	1	2	2	1	1	1	1	2	1	1
$N(E)_{\text{NIST}}$	1.1E+06	1.1E+06	1.3E+06	1.5E+05	1.7E+05	5.2E+05	1.4E+05	9.1E+05	2.0E+05	8.3E+05	2.7E+05	7.6E+05	1.6E+05	6.2E+05
$[E]_{\text{NIST}} \text{ (ng.g-1)}$	36	38.4	37.9	35.5	37.7	35.6	37.3	37.6	35.5	38.3	38	36.8	39.2	37
$L(E)_{\text{Abs}} \text{ (ag)}$	105 ag	127 ag	80 ag	707 ag	388 ag	173 ag	633 ag	85 ag	276 ag	95 ag	227 ag	114 ag	555 ag	113 ag
$L(E)_{\text{Abs for 0}} \text{ (ag)}$	34 ag	35 ag	31 ag	246 ag	223 ag	173 ag	265 ag	43 ag	183 ag	48 ag	145 ag	50 ag	258 ag	61 ag

$L(E)_{\text{Abs for 0}}$ is the minimal detection limit that could be reached if $N(E)_{\text{Blank}}=0$

Table 3 Detection limits calculated for the 14 lanthanides ($V=1.5E^{-13} \text{ m}^3$ and $\rho_{\text{NIST}}=2530 \text{ kg.m}^{-3}$)

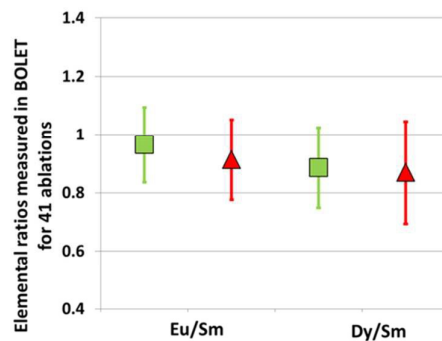


Figure 3 Elemental ratios Eu/Sm, and Dy/Sm for 41 ablations of uranium reference particles from the "Bolet" reference material. Each ratio was corrected through measurement of the same ratio with the NIST 612 reference material. Green squares represent the mean values of the measured ratios (for 41 ablations), the uncertainties represent the external reproducibility. Reference values and their uncertainties for each ratio (calculated from the given value from CETAMA, as a quadratic combination) are represented by red triangles.

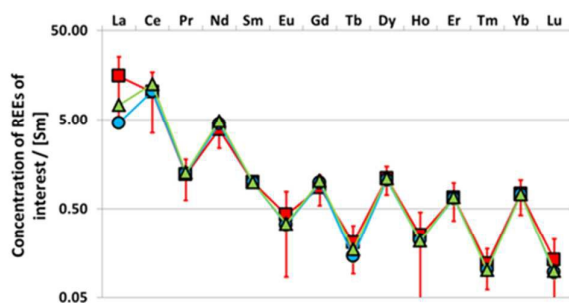


Figure 4 Comparison of relative distribution of lanthanides (normalized to the Sm concentration) in the "Olympic Dam" UOC by different methods. Micro-analyses (in red) were performed in this study by ablation of a few hundreds of ng of material by fs-LA-ICP-MS (red squares). Ratios were corrected with NIST 612. Bulk analyses were performed by separation on resin prior to the analysis by SF-ICP-MS for the two other laboratories (CEA, blue circles, and ITU, green triangles).

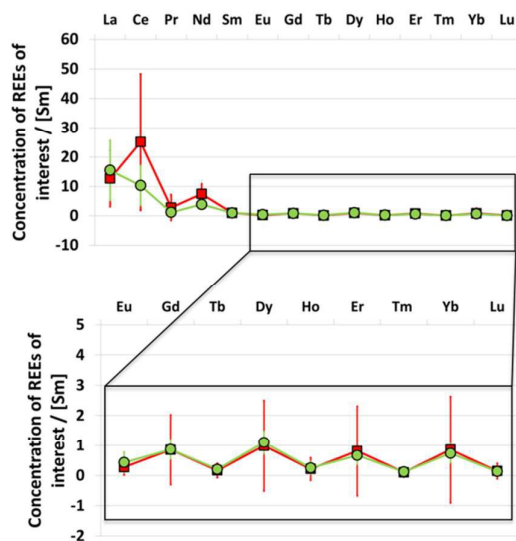


Figure 5 Comparison of relative distribution of lanthanides (normalized to Sm concentration) measured in the "Olympic Dam" UOC (this study) and in the original ore (Ciobanu et al)²⁹ by LA-ICP-MS. For the UOC (green circles), the ratios were calculated from 10 ablations of a few ng of material, and were corrected with the NIST 612 reference material. For the uranium ore (red squares) the values were obtained by calculating the mean of different ablations of REE inclusions in the ore.